Structural formation of poly(ethylene terephthalate) during the induction period of crystallization: 2. Kinetic analysis based on the theories of phase separation

M. Imai, K. Mori and T. Mizukami
Research Center, Toyobo Co. Ltd, Otsu, Shiga 520-02, Japan

and K. Kaji* and T. Kanaya
Institute for Chemical Research, Kyoto University, Uji, Kyoto-fu 611, Japan
(Received 8 August 1991; revised 26 November 1991; accepted 27 December 1991)

Crystallization processes of poly(ethylene terephthalate) (PET) when annealed at 80°C, or 5°C above the glass transition temperature, T_g, have been investigated by a small-angle X-ray scattering (SAXS) technique. At a very early stage of annealing, a scattering maximum appears at around $Q = 0.04$ Å^{-1}, where Q is the length of the scattering vector ($Q = 4\pi \sin\theta/\lambda$). During the so-called induction period of crystallization, this maximum intensity increases with annealing time and the maximum position shifts towards the low Q side. These results confirm the previously reported new finding that the long-range ordered structure is formed in the induction period before crystallization. These ordering processes can be divided into two stages: an early and a late stage. The scattering behaviour in the early stage is in accordance with the prediction of Cahn's linearized theory for spinodal decomposition. The scattering profiles in the late stage can be described in terms of Furukawa's scaling theory for the cluster growth regime. From these experimental results, we conclude that the growth process of the density fluctuation occurs in the induction period and this process is very similar to the spinodal decomposition type of phase separation process. It is considered that after this dense domain grows to a certain size, crystallization begins.

(Keywords: crystallization; induction period; small-angle X-ray scattering; spinodal decomposition; scaling theory; poly(ethylene terephthalate))

INTRODUCTION

In the previous paper[1] we investigated the crystallization processes of poly(ethylene terephthalate) (PET) when annealed at 115°C, or 40°C above the glass transition temperature, T_g, using small-angle and wide-angle X-ray scattering (SAXS and WAXS) techniques, and found that the long-range ordered structure, having a correlation length of about 200 Å, is formed in the induction period before crystallization begins. This new finding seems to be closely related to crystal nucleation, the mechanism of which has not been well understood to date.

The general theory of crystal nucleation, which was reviewed very recently by Kelton[2], is based on the assumption that phase transformation is initiated by long-amplitude, localized fluctuations of some order parameter such as density, leading to the appearance of small regions of stable crystalline phase. When these regions are larger than some critical size, they will grow and eventually crystallize the liquid. The time needed to reach the critical size of the dense regions from the disordered amorphous structure is the so-called induction period. Therefore, we consider that the long-range ordered structure observed in the induction period corresponds to this dense region.

In this paper we investigate the long-range ordering processes observed in the induction period based on the kinetics of the first-order phase transition. For this purpose, it is necessary to examine the annealing processes in more detail by employing a lower annealing temperature for the sample, and consequently a slower crystallization rate. The annealing processes of PET at 80°C, or only 5°C above T_g, have therefore been studied using the time-resolved SAXS method. Based on the observed results, we first show that the time dependence of the scattering profiles is in accordance with the predictions from the phase separation process[3]. Then we analyse the scattering profiles based on Cahn's linearized theory[4,5] and Furukawa's scaling theory[6,7] which describe the early and the late stages in the phase separation process, respectively.

EXPERIMENTAL

The PET used for this study had a number-average molecular weight, M_n, of 25 000 and a polydispersity, $M_w/M_n = 2.5$. The PET was melted at 290°C for 2 min and immediately quenched in ice–water. The density of the melt-quenched samples was 1.333 g cm^{-3}, which agrees with the value reported for amorphous PET[8]. The melt-quenched sample was annealed isothermally at 80°C

*To whom correspondence should be addressed

0032-3861/92/214457-06

in a temperature-controlled cell for SAXS measurements. The annealing processes were followed by the time-resolved SAXS measurements, which were performed on the 6 m point focusing SAXS camera at the High-Intensity X-ray Laboratory of Kyoto University[9]. Details of the experiments are described in the previous paper[1].

RESULTS

Annealing isotherm

The glass transition temperature and the melting temperature of the samples are 75°C and 250°C, respectively. *Figure 1* shows the annealing isotherm $\phi(t)$ measured by differential scanning calorimetry (d.s.c.). The isotherm at 80°C was calculated according to the equation:

$$\phi(t) = \frac{\int_0^t (\mathrm{d}H_t/\mathrm{d}t)\,\mathrm{d}t}{\int_0^\infty (\mathrm{d}H_t/\mathrm{d}t)\,\mathrm{d}t} \quad (1)$$

where $\mathrm{d}H_t/\mathrm{d}t$ is the rate of evolution of heat. The isotherm curve exhibits a sigmoidal shape typical of polymer annealing behaviour. During the initial annealing time of about 120 min, $\phi(t)$ does not change from the initial value, indicating the so-called induction period. In the induction period the sample maintains a constant density of 1.333 g cm^{-3}, the same value as that of amorphous PET. After that $\phi(t)$ increases rapidly with annealing time, which indicates the initiation of crystallization.

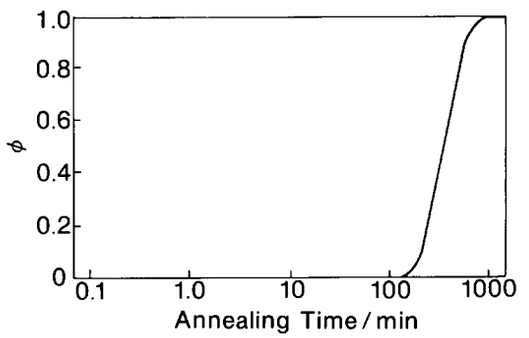

Figure 1 Annealing isotherm of the amorphous melt-quenched PET sample at 80°C

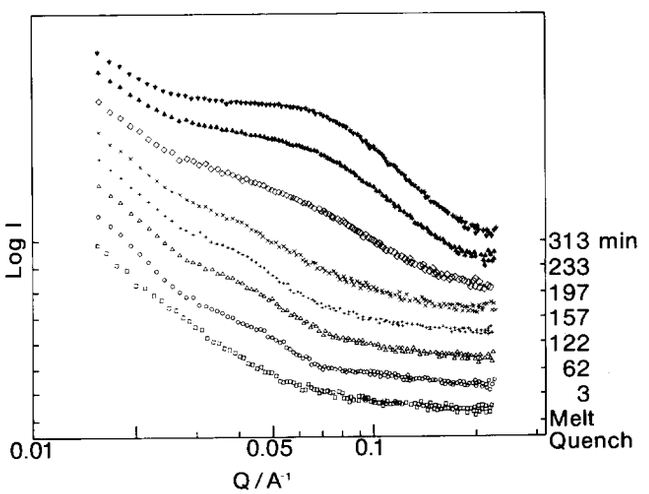

Figure 2 Small-angle X-ray scattering profiles for the melt-quenched sample and the samples annealed for 3, 62, 122, 157, 197, 233 and 313 min at 80°C

Time evolution of SAXS profiles during annealing

Figure 2 shows the time-resolved SAXS profiles at 80°C in double logarithmic form. For convenience each curve is shifted along the intensity axis. In *Figure 2*, the scattering profiles of the samples annealed for 3, 62 and 122 min correspond to the induction period and those for 157, 197, 233 and 313 min correspond to the crystallization stage. From these scattering profiles, it is noticed that after annealing for 3 min a broad peak appears near $Q = 0.04$ Å^{-1}. The intensity around this scattering peak in the Q range of 0.03–0.05 Å^{-1} increases with annealing time throughout the induction period. This reconfirms the surprising fact, reported previously, that the ordering processes of long-range scale (about 150 Å in this case) begin at a very early stage of the induction period, while the macroscopic amorphous density of the system remains unchanged during this period. After the induction period, a new scattering peak corresponding to the usual long period appears near $Q = 0.06$ Å^{-1}, increasing in intensity with time. In order to analyse the scattering profiles in more detail, we subtracted the intensity of the melt-quenched sample from those of the annealed samples; the results are shown in *Figure 3*. *Figure 3a* shows the difference scattering profiles for the samples annealed for 3–122 min, being within the induction period before crystallization. This figure clearly shows that the single scattering maximum appears at around $Q = 0.04$ Å^{-1}, immediately after the initiation of annealing. As the annealing time increases, the maximum position shifts towards smaller Q simultaneously with increasing the maximum intensity. *Figure 3b* shows the difference profiles for the samples annealed for 122–197 min, corresponding to the intermediate stage from the end of the induction period to the initiation of crystallization. The scale of the ordinate in *Figure 3b* is contracted by five times that in *Figure 3a*. During the annealing time of 122–157 min, the maximum intensity increases with time as the maximum position shifts to $Q = 0.02$ Å^{-1}. The scattering profile after annealing for more than 197 min exhibits no intensity maximum in the observed Q range; it may be below the observable lower limit. On the other hand, the scattering intensity in the vicinity of $Q = 0.06$ Å^{-1} begins to increase owing to the appearance of the so-called long-period structure. *Figure 3c* shows the difference of the so-called long-period structure. *Figure 3c* shows the difference profiles for the samples annealed for 197–313 min, corresponding to the crystallization process. In these scattering profiles, the peak intensity of the long period structure increases remarkably with annealing time. In the low Q range, no characteristic change is observed because the peak maximum may be outside the Q range of the diffractometer. All the results described above reconfirm the results of the previous paper[1] where annealing was performed at 115°C. In this paper, however, the data obtained are more precise so that further detailed analyses are possible based on the theories described in the Introduction.

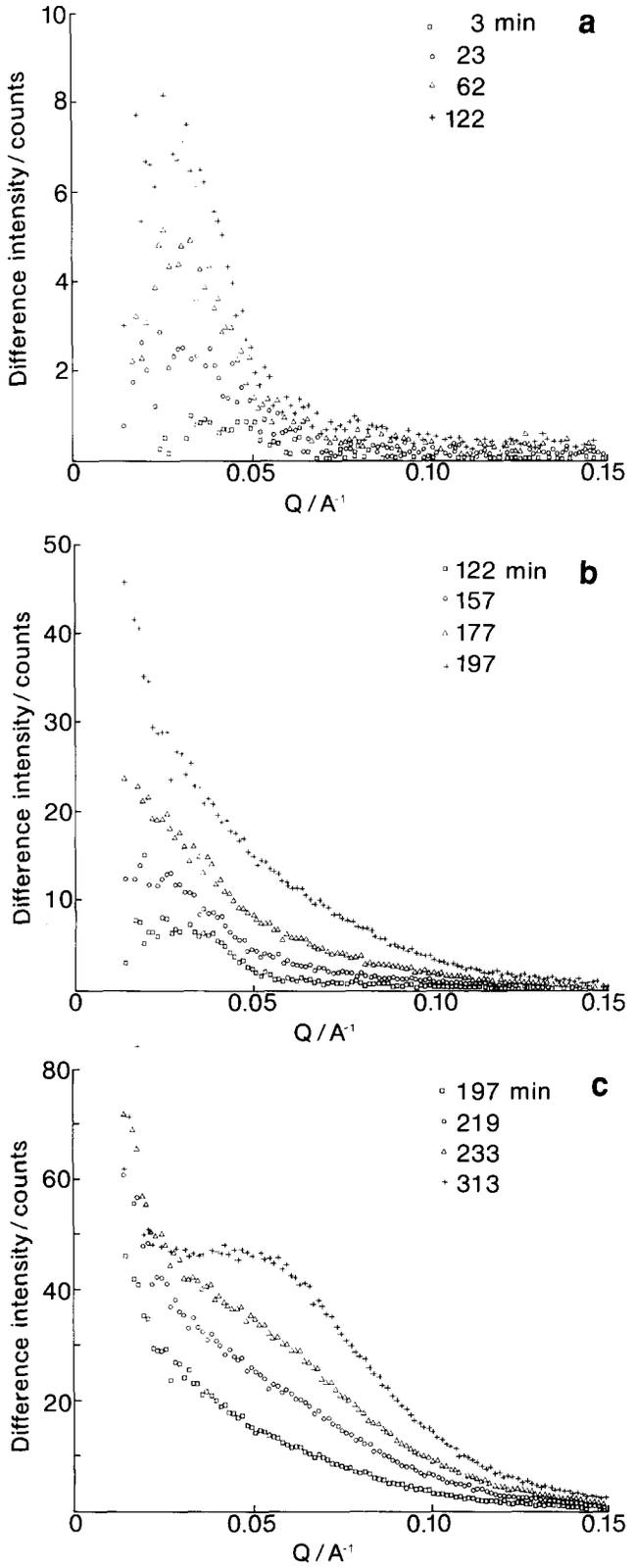

Figure 3 Difference scattering intensity profiles of the annealed samples after subtraction of the profile of the melt-quenched sample. Annealing time: (a) 3–122 min; (b) 122–197 min; (c) 197–313 min

ANALYSIS OF ANNEALING PROCESSES IN THE INDUCTION PERIOD OF CRYSTALLIZATION

From the experimental results, it is apparent that the long-range ordered structure is formed and grows during the induction period while the macroscopic density of the system does not change. It is very surprising that the observed time evolution of the scattering profiles during the induction period resembles the results observed for the spinodal decomposition type of phase separation process. Therefore, we analyse the scattering data obtained based on the kinetics of phase separation[3]. To show the applicability of the kinetics of phase separation, we first plot the time evolution of the scattering intensity and the scattering peak position Q_m during the induction period, as shown in *Figures 4* and *5*, respectively. It should be noted from these figures that during the induction period two stages of structural formation exist. In the early stage, corresponding to the time-scale up to 20 min, the intensity increases exponentially with time while the peak position does not change. In the late stage, corresponding to the time-scale from 30 to 120 min, the intensity increases gradually while the peak position shifts to the lower Q side. However, an intermediate stage seems to be distinguishable between 20 and 30 min, where the scattering intensity increases exponentially with time while the peak position begins to shift towards the lower Q side. These features agree well with the scattering behaviour in the spinodal decomposition of a blend system[10]. In order to elucidate the structural formation during the induction period, we examine the behaviour of the scattering profiles in the early stage and the late stage in terms of Cahn's linearized theory[4,5] and Furukawa's scaling theory[6,7], respectively.

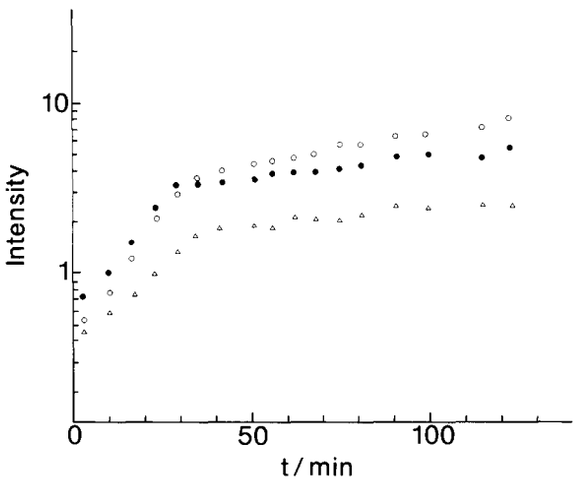

Figure 4 Annealing time t dependence of the scattering intensity as a function of Q during the induction period before crystallization. Q values ($Å^{-1}$): ○, 0.03; ●, 0.04; △, 0.05

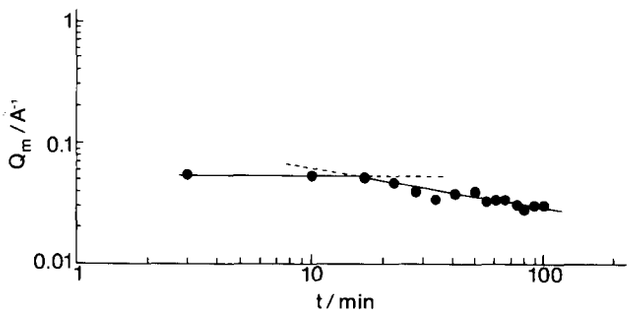

Figure 5 Annealing time t dependence of the wavenumber Q_m at maximum intensity

Analysis of the early stage by Cahn's linearized theory

In the initial stage, the scattering functions have the following three features: (1) the scattering maximum appears; (2) the peak position scarcely changes; (3) the peak intensity increases exponentially with annealing time. Interpreting these features by Cahn's linearized theory[4,5], the flux of the density is given by:

$$\frac{\partial \rho}{\partial t} = D_c(\partial^2 f/\partial \rho^2)\nabla^2 \rho - 2D_c \kappa \nabla^4 \rho + \cdots \quad (2)$$

where ρ is density, D_c is the translational diffusion constant, f is the free energy density of the system and κ is a positive constant. The solution of equation (2) is:

$$\rho(R) - \rho_0 = \sum_Q \exp[R(Q)t]\{A(Q)\cos(QR) + B(Q)\sin(QR)\} \quad (3)$$

where $R(Q)$ corresponds to the growth rate of the density fluctuation given by:

$$R(Q) = D_c Q^2\{-(\partial^2 f/\partial \rho^2) - 2\kappa Q\} \quad (4)$$

and $A(Q)$ and $B(Q)$ are constants. As shown below, the most important point is that the scattering maximum appears only for the phase separation in the unstable region where spinodal decomposition occurs and not in the metastable region where nucleation growth occurs. In the metastable region $R(Q)$ is negative since $\partial^2 f/\partial \rho^2$ is positive and κ is positive, so that the amplitude of density fluctuation cannot grow but rather disappears. In the unstable region $\partial^2 f/\partial \rho^2$ is negative and hence $R(Q)$ can be positive for some Q range, as seen from equation (4). Then the fluctuation within such a Q range can grow with time and gives a scattering maximum. In this case, the scattering peak position Q_m does not change and the intensity $I(Q)$ increases exponentially with time:

$$Q_m^2 = -(\partial^2 f/\partial \rho^2)/4\kappa \quad (5)$$

$$I(Q,t) = I(Q,0)\exp[2R(Q)t] \quad (6)$$

In other words the characteristic wavelength of the fluctuation is independent of time and the amplitude of the fluctuation increases exponentially with time during the early stage. These predictions of Cahn's linearized theory for the spinodal decomposition actually agree with the experimental results observed in the early stage, as shown in *Figures 4* and *5*. The characteristic wavelength is about 150 Å and the maximum growth rate $R(Q_m)$ is about $5.0 \times 10^{-4}\ s^{-1}$.

Analysis of the late stage by Furukawa's scaling theory

In the late stage, Q_m starts to decrease with annealing time; the characteristic wavelength of fluctuations in spinodal decomposition increases with time and the intensity starts to deviate from the exponential increase as the intensity tends to increase more slowly. These features are in accordance with predictions from the late stage of spinodal decomposition, i.e. that the amplitude of the fluctuation reaches the equilibrium value and the characteristic size of the domain grows keeping a self-similarity. Therefore, we apply the dynamic scaling theory developed by Furukawa[6,7] to this late stage, which describes the cluster growth process in terms of the cluster diffusion and reactions by assuming that the structure function $S(Q,t)$ can be scaled with a single length parameter $R(t)$ as:

$$S(Q,t) \sim R^d(t)\tilde{S}(x) \quad (7)$$

where d is the dimensionality of the system, $\tilde{S}(x)$ is a universal scaling function given by:

$$\tilde{S}(x) = \frac{x^2}{(\gamma/2) + x^{2+\gamma}} \quad (8)$$

x being defined as

$$x = QR(t) \quad (9)$$

and γ being defined as:

$$\gamma = \begin{cases} d+1 & \text{for cluster regime} \\ 2d & \text{for percolation regime} \end{cases} \quad (10)$$

Furukawa also assumes that the characteristic size changes as:

$$R(t) \propto t^a \quad (11)$$

Equations (7)–(11) for the cluster regime give the wave vector Q_m at the maximum intensity and the maximum intensity I_m as follows:

$$Q_m(t) \sim R^{-1}(t) \propto t^{-a} \quad (12)$$

$$I_m(t) \sim R^3(t) \propto t^b \quad (13)$$

where

$$b/a = d = 3 \quad (14)$$

Figure 5 shows that changes in the value of Q_m obey the power law of equation (12) in the late stage ranging from 30 to 120 min. As shown in *Figure 6*, the annealing time dependence of I_m in the late stage can also be described by the power law of equation (13). The exponents a and b are estimated in the region of the late stage, corresponding to the time range of 30–120 min of *Figures 5* and *6*. The values of a and b are 0.25 and 0.75, respectively, by least mean square fitting of the obtained data. The ratio b/a is 3.0, which is in good agreement with the theoretical value of equation (14) or the dimensionality of the system.

In the following, we examine the observed scattering functions in terms of the scaling function. From equations (7), (12) and (14) the observed scattering intensity $I(Q,t)$ can be related to $\tilde{S}(x)$ by

$$\tilde{S}(x) \sim Q_m^3(t)I(Q,t) \quad (15)$$

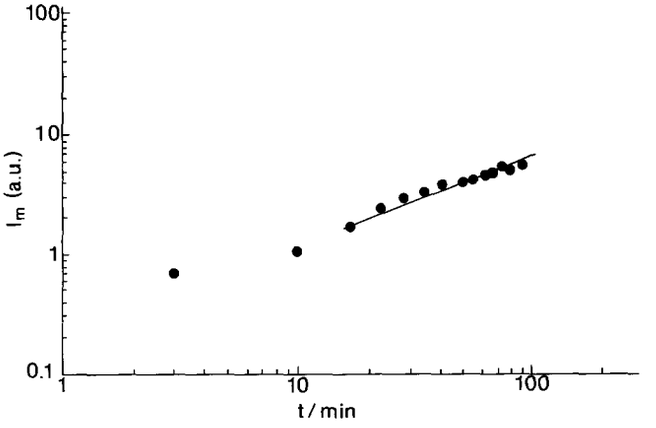

Figure 6 Annealing time t dependence of the maximum intensity I_m

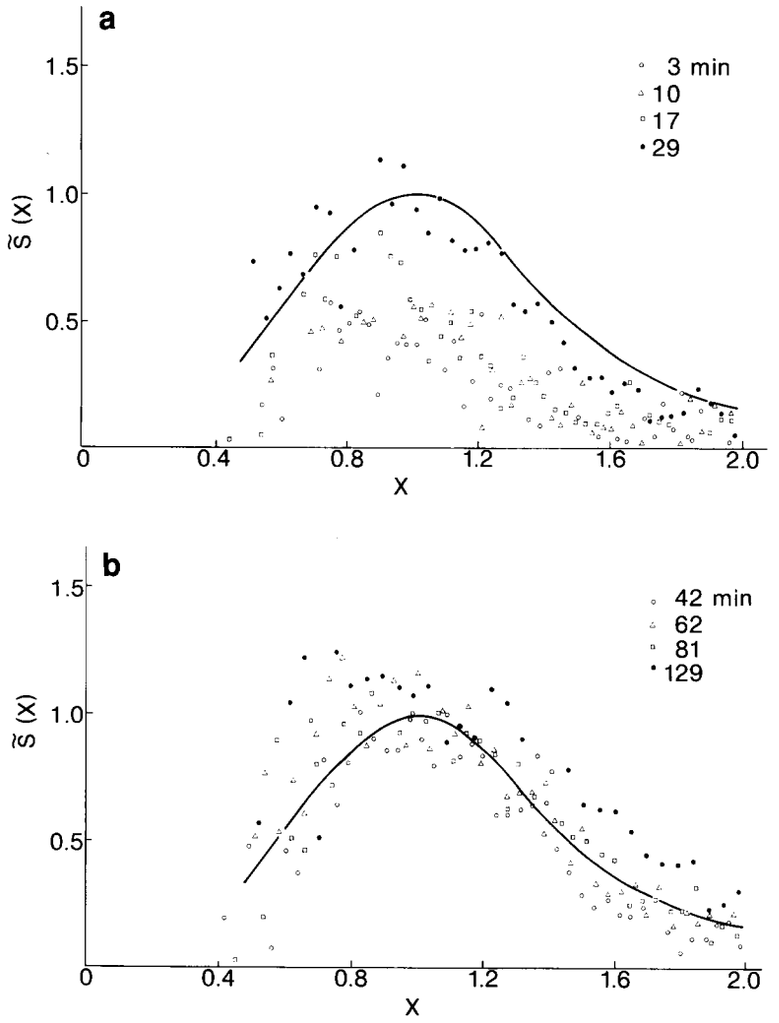

Figure 7 Observed scaled structure function $\tilde{S}(x)$ calculated by equation (15) for the annealed sample in the range of 3–29 min (a) and 42–129 min (b) at 80°C. The solid curve indicates the theoretical $\tilde{S}(x)$ of equation (8)

where $x = Q/Q_m(t)$. Using equation (15) we calculated the scaled scattering functions $\tilde{S}(x)$ in the time range of 3–129 min and compared them with equation (8). The results are plotted in *Figure 7*, in which the solid curves indicate the theoretical scaling function when $\gamma = 4$ for the cluster regime. *Figures 7a* and *b* correspond to the early and the late stages, respectively. The calculated $\tilde{S}(x)$ in the late stage appears to be independent of annealing time t and agrees with Furukawa's theoretical scaling function with the normalizing condition $\tilde{S}(1) = 1$. Here we should note that for the large x region, $\tilde{S}(x)$ can be described by the exponent $\gamma = d + 1 = 4$ rather than $\gamma = 2d = 6$. In order to clarify this result, we estimate the exponent γ using a double logarithmic plot of $\tilde{S}(x)$ because a simple relation of $\tilde{S}(x) \sim x^{-\gamma}$ can be expected for sufficiently large x from equation (8). The plot for the 35 min annealed sample is shown in *Figure 8* as an example. The exponent γ evaluated from the slope is about 4. *Figure 9* shows the time dependence of exponent γ in the induction period. In the late stage, γ has a value of about 4 corresponding to Porod's law[11], indicating the formation of a smoothly curved boundary. Therefore the structure formation in this stage can be described in terms of the cluster growth process.

On the other hand, the observed structure functions $\tilde{S}(x)$ in the early stage increase with annealing time and

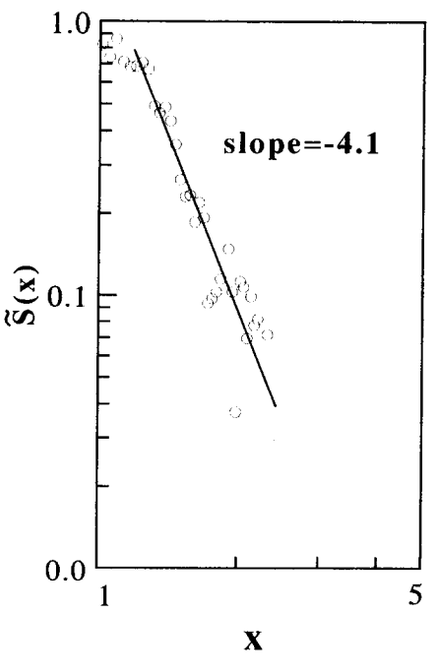

Figure 8 Double logarithmic plot of $\tilde{S}(x)$ for 35 min annealed sample

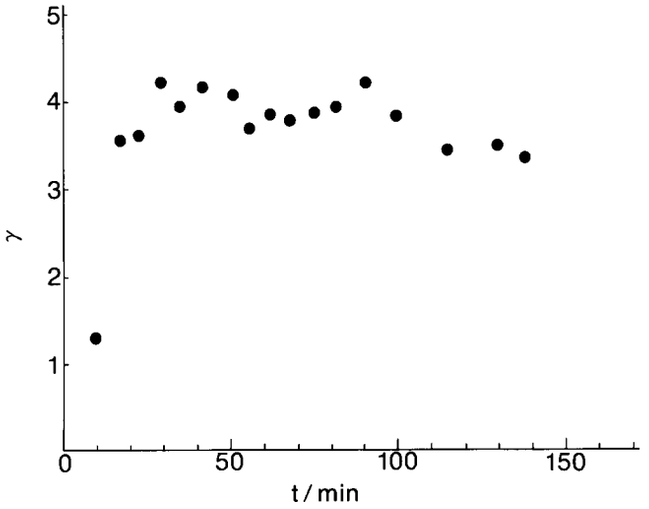

Figure 9 Annealing time t dependence of the exponent γ as defined by equation (10)

cannot be described by the theory. In Furukawa's cluster theory, the mean squared density fluctuation in the cluster is assumed to be constant. However, it is considered that in the early stage of the induction period, the amplitude of fluctuation in the cluster does not yet reach the equilibrium value, but increases with annealing time. Hence it seems that the scattering functions cannot be scaled by a single cluster size parameter.

DISCUSSION

As described in the Introduction, in order to form the critical crystal nucleus it is necessary for the long range density fluctuations to grow to a certain value, i.e. the critical size. We consider that the observed time evolution of scattering profiles in the induction period reflects this growth process. We have examined the data obtained in terms of the kinetics of the first order phase transition. The phenomenological equation for this kinetics is:

$$\partial S/\partial t = -L(\partial A/\partial S) \tag{16}$$

$$L = L_0(-i\nabla)^{\alpha} \tag{17}$$

$$\alpha = \begin{cases} 0 & \text{for non-conserved system} \\ 2 & \text{for conserved system} \end{cases}$$

where S is the order parameter, L is the phenomenological kinetic coefficient and A is free energy. The equation for conserved system, i.e. spinodal decomposition type of phase separation, describes the observed profiles well when we adopt the local density as the order parameter S. These analytical results do not necessarily mean that the phase separation process occurs during the induction period, but they do mean that the free energy function $A(\rho)$ for the induction period apparently has a very similar form to that for the spinodal decomposition type of phase separation process, which has two local minima. It is considered that crystal nucleation is a thermally activated process and the initial amorphous state is within the metastable region[2]. However, our experimental results suggest that the initial amorphous state is unstable and only after the formation of a certain long-range ordered structure producing the local potential minimum does the activated process of crystallization take place. This means that the function $A(\rho)$ is somewhat modified from the usual activation process of crystal nucleation. We consider that this modification of $A(\rho)$ may be due to topological and steric effects of the polymer chains, such as entanglements, which obstruct the complete crystallization of the bulk polymers.

CONCLUSIONS

The ordering processes when the amorphous PET was annealed just above the glass transition temperature, were investigated using a SAXS method. First, the new finding reported in the previous paper[1] was reconfirmed, i.e. that the long-range ordered structure is formed in the induction period before crystallization. Further, it was made clear that these ordering processes can be divided into two stages, the early stage and the late stage. We analysed the scattering data obtained, based on the kinetics of phase separation because the order parameter of the system is conserved in the induction period. The scattering behaviour in the early stage can be described by Cahn's linearized theory for spinodal decomposition. The scattering profiles in the late state can be described in terms of Furukawa's scaling theory; the universal structure factor for the growth process of clusters fits the experimental data excellently. From these experimental results, we conclude that the dense region is formed in the induction period and this structure formation process is very similar to the spinodal decomposition type of phase separation process. It is considered that after this dense region grows to a certain size, crystallization begins.

ACKNOWLEDGEMENTS

We thank the Committee of the High Intensity X-ray Laboratory of Kyoto University for the small-angle X-ray scattering system. We would also like to express our sincere thanks to Dr H. Hayashi and Dr S. Suehiro for experimental support and helpful discussions.

REFERENCES

1 Imai, M., Mori, K., Mizukami, T., Kaji, K. and Kanaya, T. *Polymer* 1992, **33**, 4451
2 Kelton, K. F. in 'Solid State Physics' (Eds H. Ehrenreich and D. Turnbull), Vol. 45, Academic Press, New York, 1991
3 Gunton, J. D., Miguel, M. S. and Sahni, P. S. in 'Phase Transitions and Critical Phenomena' (Eds C. Domb and J. L. Lebowitz), Vol. 8, Academic Press, New York, 1983
4 Cahn, J. W. and Hilliard, J. E. *J. Chem. Phys.* 1958, **28**, 258
5 Cahn, J. W. *J. Chem. Phys.* 1965, **42**, 93
6 Furukawa, H. *Physica* 1984, **123A**, 497
7 Furukawa, H. *Adv. Phys.* 1985, **34**, 703
8 Fischer, E. W. and Fakirov, S. *J. Mater. Sci.* 1976, **11**, 1041
9 Hayashi, H., Hamada, F., Suehiro, S., Masaki, N., Ogawa, T. and Miyaji, H. *J. Appl. Cryst.* 1988, **21**, 330
10 Hashimoto, T., Kumaki, T. and Kawai, H. *Macromolecules* 1983, **16**, 641
11 Porod, G. *Kolloid-Z.* 1951, **124**, 83